PERGAMON

International Journal of Solids and Structures 39 (2002) 617–635

INTERNATIONAL JOURNAL OF SOLIDS and STRUCTURES

www.elsevier.com/locate/ijsolstr

A general vibration model of angle-ply laminated plates that accounts for the continuity of interlaminar stresses

Arcangelo Messina [a,*], Kostas P. Soldatos [b]

[a] *Dipartimento di Ingegneria dell'Innovazione, Università di Lecce, Via Monteroni, 73100 Lecce, Italy*
[b] *University of Nottingham, Pope Building, Nottingham NG7 2RD, UK*

Received 1 November 2000

Abstract

This paper presents the generalisation of a well documented two-dimensional shear deformable laminated shell theory [Compos. Struct. 25 (1993) 165] that, based on a fixed number of unknown variables, was initially proposed for laminates made of specially orthotropic layers only. The theory is here specialised for laminated plates but is able to encompass monoclinic layers in a general multilayered configuration. Moreover, it is able to account for the interlaminar continuity of both displacements and transverse shear stresses. Higher-order effects, as shear deformation and rotary inertia, are naturally included into the formulation. In order to obtain the relevant governing differential equations, both Hamilton's variational principle and a recently proposed vectorial approach [Compos. Engng. 3 (1993) 3] have been independently used. The effectiveness of the present model is tested numerically by comparing its results with exact three-dimensional elasticity results obtained under the particular condition that the plates vibrate in cylindrical bending.

Keywords: Free vibration analysis; Laminated composite; Continuity interlaminar stresses; Higher order theories

1. Introduction

The two-dimensional (2D) laminated plate theories available in the literature are the so-called layer-wise theories, the number of the degrees of freedom of which depends on the number of layers, and theories that use a fixed number of degrees of freedom regardless of the number of layers involved. It appears that the first attempts to incorporate interlaminar stress continuity into a displacement-based, shear deformable, laminated plate model of the later class are due to Sun and Whitney (1973) and Chou and Carleone (1973). Both studies assumed a displacement field similar to the displacement approximation used for the so-called uniform shear deformable plate theory (USDPT) (Yang et al., 1966; Whitney and Pagano, 1970). However, though Chou and Carleone (1973) used the USDPT displacement field throughout the whole thickness of

* Corresponding author. Fax: +39-832-320-279.
E-mail address: arcangelo.messina@unile.it (A. Messina).

0020-7683/02/$ - see front matter
PII: S0020-7683(01)00169-X

the laminate, Sun and Whitney (1973) assumed such a displacement field in a layer-wise sense. By accounting for the interlaminar continuity of both displacements and transverse shear stresses, Sun and Whitney (1973) were next able to express the plate energy functional in terms of five degrees of freedom only, but they did not present explicit expressions of the corresponding equations of motion.

The leading assumption in Chou and Carleone (1973) was the simplification that transverse shear stresses are distributed uniformly throughout the thickness of a laminated plate. This assumption, led Chou and Carleone (1973) to an indirect, a posteriori, modification of the governing differential equations of USDPT that improves displacement and stress predictions. It should be noted, however, that the improvement in the performance of the USDPT was detected by means of comparisons with exact elasticity results obtained for cross-ply laminates only subjected to cylindrical bending (Pagano, 1969). Although the theoretical models involved in both Sun and Whitney (1973) and Chou and Carleone (1973) appear to be applicable to laminates having general angle-ply stacking patterns, neither of the related analyses was applied beyond the relatively simple pattern of a cross-ply lay-up.

Di Sciuva (1986) introduced a five degrees of freedom, USDPT-based laminated plate model which, upon assuming a through-thickness piecewise linear distribution of the in-plane displacements in each layer, allows the interlaminar continuity of both displacements and transverse shear stresses to be satisfied. Though the model appeared to be equivalent to that of Chou and Carleone (1973), all the relevant assumptions were done ab initio and the governing equations were consistently obtained, on a variational basis, together with the related boundary conditions. This model (Di Sciuva, 1986) was introduced for plates made of specially orthotropic layers. Further results and improvements were subsequently presented in Di Sciuva (1987, 1992), He et al. (1993) and He and Ma (1994), but again numerical applications did not proceed beyond the cross-ply stacking pattern. It should be noted that the models presented in all (Sun and Whitney, 1973; Chou and Carleone, 1973; Di Sciuva, 1987) are unable to inherently satisfy the shear traction boundary conditions imposed on the lateral (top and bottom) plate planes and, therefore, require the use of transverse shear correction factors. Contrary to this, the relevant models introduced by He et al. (1993) and He and Ma (1994) appear capable to satisfy zero shear traction boundary conditions on those lateral surfaces and, hence, they avoid the undesirable implications of shear correction factors. These models, introduce however a considerable number of additional algebraic equations, which are coupled with the differential equation of motion and have to be solved on an iterative basis.

The so-called parabolic, shear deformable plate models fulfil the zero shear traction lateral boundary conditions at the top and at the bottom of the laminate and hence avoid the use of transverse shear correction factors. Their original version (Bhimaraddi and Stevens, 1984; Reddy, 1984; Soldatos, 1988) makes also use of five degrees of freedom but violates the interlaminar stress continuity conditions. One of the first attempts to account for a parabolic distribution of the transverse shear stresses and simultaneously to fulfil their interlaminar continuity requirements, appears to be due to Ren (1986a,b). This static model that was later extended (Ren and Owen, 1989), to encompass also dynamic analysis of cross-ply and angle-ply laminates, made finally use of seven degrees of freedom. Some numerical results for angle-ply stacking patterns were also obtained on the basis of that model (Ren and Owen, 1989) but no comparisons with relevant exact elasticity results were made. Successful attempts towards the development of a five degrees of freedom parabolic shear deformable plate theory (PSDPT) that also fulfils the continuity requirements of the interlaminar shear stresses were later presented in Lee et al. (1990, 1993, 1994), Savithri and Varadan (1990a,b), Di Sciuva (1992) and Cho and Parmerter (1992, 1993) none of which however presented numerical results dealing with the dynamics of angle-ply laminated plates.

At this point, the recent studies by Librescu and Lin (1996, 1999) and Librescu et al. (1997) should be mentioned. These studies were mainly oriented to substantiate the implications of the violation of the interlaminar shear stress continuity requirements on the predictions of the mechanical response characteristics of certain simply supported plates and shells made of transversally isotropic layers. Librescu and Lin (1996), in particular, showed how the global characteristics response, obtained by means of a model

that violates these continuity requirements, can result into an underprediction/overprediction of the corresponding global responses based on (what should be) a more accurate model that fulfils these continuity requirements. These observations that were also reinforced in relevant studies by Soldatos and Messina (1998) and Messina and Soldatos (1999a,b), suggested that further relevant investigations would be useful in connection with the dynamic behaviour of angle-ply laminates.

In this context, this paper, initially presents a further generalisation of a well documented displacement-based 2D shear deformable laminate theory (Soldatos and Timarci, 1993) in a manner that makes possible the consideration of continuous interlaminar stresses in angle-ply laminates. Accordingly, the theory, which uses only five unknown displacement functions, is able to account for the continuity of interlaminar shear stresses in laminated plates made of monoclinic layers in a general stacking pattern of material arrangement. Its governing equations of motion are consistently obtained by using a new generalised vectorial approach (Soldatos, 1993) but also by applying Hamilton's variational principle. In the later case the full set of relevant boundary conditions are also obtained.

The effectiveness of such an extended 2D dynamical model thus obtained is then verified by comparing its natural frequency predictions with corresponding predictions due to exact three-dimensional (3D) elasticity analysis. Such exact, 3D elasticity results are obtained by carrying out an appropriate dynamic extension of the corresponding static, cylindrical bending solution due to Pagano (1970). These comparisons yield some valuable physical insights that, due to ascertained underpredictions/overpredictions of natural frequencies between the presented model and the exact 3D one, illustrate a necessity to look for new shape functions that in some cases might model more accurately the in-plane displacement distributions throughout the thickness of a laminate.

2. Theoretical modelling

Consider a rectangular plate having a constant thickness h, axial length L_x and width L_y (Fig. 1). The in-plane and normal to the middle-plane co-ordinate length parameters are denoted with x, y and z, respectively, whereas U, V and W represent the corresponding displacement components. Fig. 1 depicts two particular cases of laminated plates, with odd or even number of layers that will later be employed in example applications. These are the cases of plates having a so-called regular symmetric and regular antisymmetric angle-ply lay-up, respectively; they both involve laminates made of generally orthotropic layers of the same thickness, h/L (Jones, 1975). Accordingly, in each layer, one of the three principal material axes of orthotropy lies on a plane parallel to the plate middle-plane (x–y plane) and makes a certain angle, θ, with the x-axis of the adopted Cartesian co-ordinate system.

An explicit form of the elastic laws that governs the plate material will not be provided at this stage. Instead, and in a close connection with the formulation presented initially in Soldatos (1988) and generalised later in Soldatos (1993), it is more generally assumed that there exists a strain energy density function $V_0(\varepsilon_x, \varepsilon_y, \varepsilon_z, \gamma_{yz}, \gamma_{xz}, \gamma_{xy})$ such that,

$$\left(\sigma_x, \sigma_y, \sigma_z, \tau_{yz}, \tau_{xz}, \tau_{xy}\right) = \left(\frac{\partial V_0}{\partial \varepsilon_x}, \frac{\partial V_0}{\partial \varepsilon_y}, \frac{\partial V_0}{\partial \varepsilon_z}, \frac{\partial V_0}{\partial \gamma_{yz}}, \frac{\partial V_0}{\partial \gamma_{xz}}, \frac{\partial V_0}{\partial \gamma_{xy}}\right). \tag{1}$$

Under these considerations, the present shear deformable, elastic plate model begins with the following displacement approximation:

$$\begin{aligned} U(x,y,z;t) &= u(x,y;t) - zw_{,x} + \Phi_1(z)u_1(x,y;t) + \Phi_3(z)v_1(x,y;t), \\ V(x,y,z;t) &= v(x,y;t) - zw_{,y} + \Phi_2(z)v_1(x,y;t) + \Phi_4(z)u_1(x,y;t), \\ W(x,y,z;t) &= w(x,y;t), \end{aligned} \tag{2}$$

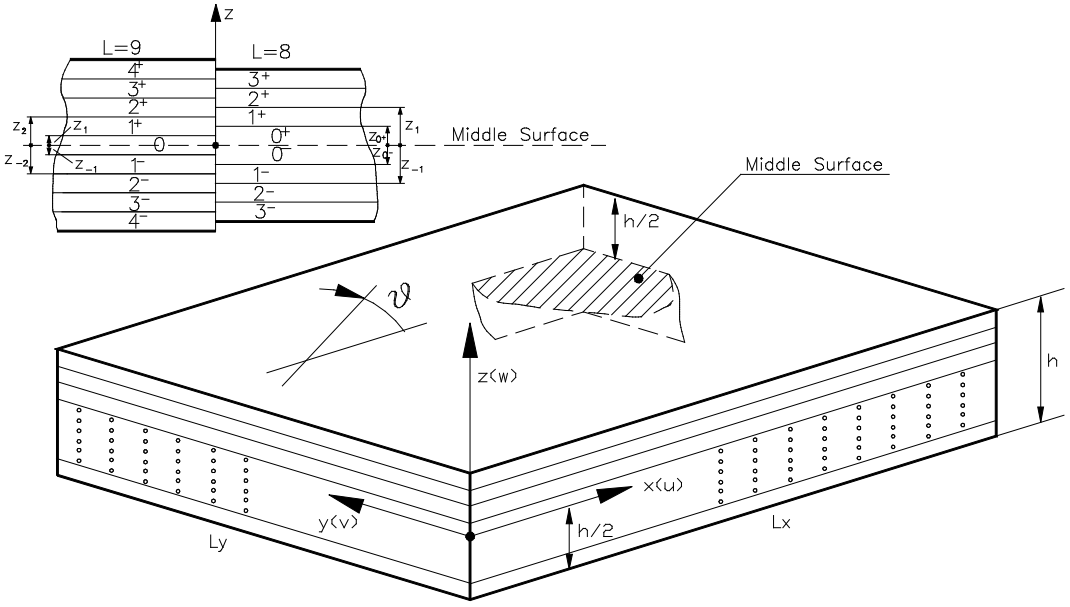

Fig. 1. Notation used for the 2D modelling of symmetric or antisymmetric laminated plates.

where t denotes time. Upon then applying the strain–displacement equations of 3D elasticity, one obtains the following kinematic relations:

$$\begin{aligned}
\varepsilon_x &= e_x + zk_x^c + \Phi_1 k_x^a + \Phi_3 k_{yx}^a,\\
\varepsilon_y &= e_y + zk_y^c + \Phi_2 k_y^a + \Phi_4 k_{xy}^a, \quad \varepsilon_z = 0,\\
\gamma_{xy} &= e_{xy} + zk_{xy}^c + \Phi_1 k_{xy}^a + \Phi_2 k_{yx}^a + \Phi_3 k_y^a + \Phi_4 k_x^a,\\
\gamma_{xz} &= \Phi_1' e_{xz}^a + \Phi_3' e_{yz}^a, \quad \gamma_{yz} = \Phi_2' e_{yz}^a + \Phi_4' e_{xz}^a,
\end{aligned} \tag{3}$$

where a prime denotes ordinary differentiation with respect to the transverse co-ordinate $((\ )' = (\mathrm{d}/\mathrm{d}z)(\ ))$ and,

$$\begin{aligned}
e_x &= u_{,x}, \quad k_x^c = -w_{,xx}, \quad k_x^a = u_{1,x}, \quad k_{yx}^a = v_{1,x},\\
e_y &= v_{,y}, \quad k_y^c = -w_{,yy}, \quad k_y^a = v_{1,y}, \quad k_{xy}^a = u_{1,y},\\
e_{xy} &= u_{,y} + v_{,x}, \quad k_{xy}^c = -2w_{,xy}, \quad e_{xz}^a = u_1, \quad e_{yz}^a = v_1.
\end{aligned} \tag{4}$$

The displacement approximation (2) still contains five unknown displacement functions, three of which (u, v and w) represent the middle-plane displacement components and have therefore the dimensions of length. As it also becomes clear from Eq. (4), the other two unknown functions (u_1 and v_1) are still related to the values that the transverse shear strains acquire on the plate middle plane and are therefore assumed to be dimensionless quantities. The introduction however of four global shape functions $\Phi_i(z)$ $(i = 1, \ldots, 4)$, which are supposed to be determined a-posteriori and should evidently have dimensions of length, is the mathematical description of the fact that the transverse shear strains γ_{xz} and γ_{yz} may be interrelated if

the complexity of the plate material exceeds the bounds of special orthotropy. In this respect, the last two of Eq. (3) imply that, for any fixed value of z, there may be a linear dependence of the of γ_{xz} and γ_{yz} values. Moreover, the pattern of this dependence through the plate thickness is dictated by the derivatives of the new shape functions $\Phi_3(z)$ and $\Phi_4(z)$ that appear in the displacement approximation (2). Hence, the displacement approximation of the previous relevant plate models (Soldatos, 1988; Soldatos and Timarci, 1993; Timarci and Soldatos, 1995) is obtained as a particular case of Eq. (2) by nullifying $\Phi_3(z)$ and $\Phi_4(z)$. Alternatively, but in mathematical terms equivalently, that previous displacement approximation, which is more suitable for cross-ply laminates, can be obtained by setting,

$$\Phi_1(z) = -\Phi_3(z), \quad \Phi_2(z) = \Phi_4(z). \tag{5}$$

With this transformation, the difference and the sum of the unknown functions u_1 and v_1 are essentially assigned to represent the values of γ_{xz} and γ_{yz} values, respectively, on the middle plane of a plate with specially orthotropic layers.

Following the procedure presented initially in Soldatos (1988) and generalised later in Soldatos (1993), the generalised force and moment resultants associated with the present elastic plate model are defined as follows:

$$\begin{aligned}
\left(N_x^c, N_y^c, N_{xy}^c\right) &= \int_{-h/2}^{h/2} \left(\frac{\partial V_0}{\partial e_x}, \frac{\partial V_0}{\partial e_y}, \frac{\partial V_0}{\partial e_{xy}}\right) \mathrm{d}z, \\
\left(M_x^c, M_y^c, M_{xy}^c\right) &= \int_{-h/2}^{h/2} \left(\frac{\partial V_0}{\partial k_x^c}, \frac{\partial V_0}{\partial k_y^c}, \frac{\partial V_0}{\partial k_{xy}^c}\right) \mathrm{d}z, \\
\left(M_x^a, M_y^a, M_{xy}^a, M_{yx}^a\right) &= \int_{-h/2}^{h/2} \left(\frac{\partial V_0}{\partial k_x^a}, \frac{\partial V_0}{\partial k_y^a}, \frac{\partial V_0}{\partial k_{xy}^a}, \frac{\partial V_0}{\partial k_{yx}^a}\right) \mathrm{d}z, \\
\left(Q_x^a, Q_y^a\right) &= \int_{-h/2}^{h/2} \left(\frac{\partial V_0}{\partial e_{xz}^a}, \frac{\partial V_0}{\partial e_{yz}^a}\right) \mathrm{d}z.
\end{aligned} \tag{6}$$

With the use of Eqs. (1) and (3), as well as the chain rule of partial differentiation, it can then be shown that these definitions are equivalent to the following:

$$\begin{aligned}
\left(N_x^c, N_y^c, N_{xy}^c\right) &= \int_{-h/2}^{h/2} \left(\sigma_x, \sigma_y, \tau_{xy}\right) \mathrm{d}z; \\
\left(M_x^c, M_y^c, M_{xy}^c\right) &= \int_{-h/2}^{h/2} \left(\sigma_x, \sigma_y, \tau_{xy}\right) z \, \mathrm{d}z; \\
\begin{bmatrix} M_x^a & M_{xy}^a \\ M_{yx}^a & M_y^a \end{bmatrix} &= \int_{-h/2}^{h/2} \begin{bmatrix} \Phi_1 & \Phi_4 \\ \Phi_3 & \Phi_2 \end{bmatrix} \begin{bmatrix} \sigma_x & \tau_{xy} \\ \tau_{xy} & \sigma_y \end{bmatrix} \mathrm{d}z; \\
\begin{bmatrix} Q_x^a \\ Q_y^a \end{bmatrix} &= \int_{-h/2}^{h/2} \begin{bmatrix} \Phi_1' & \Phi_4' \\ \Phi_3' & \Phi_2' \end{bmatrix} \begin{bmatrix} \tau_{xz} \\ \tau_{yz} \end{bmatrix} \mathrm{d}z.
\end{aligned} \tag{7}$$

Under these considerations, application of either Hamilton's principle or the generalised vectorial approach presented in Soldatos (1993) yields the following equations of motion:

$$
\begin{aligned}
&N^c_{x,x} + N^c_{xy,y} = \rho_0 \ddot{u} - \rho_1 \ddot{w}_{,x} + \rho_0^{11} \ddot{u}_1 + \rho_0^{31} \ddot{v}_1,\\
&N^c_{y,y} + N^c_{xy,x} = \rho_0 \ddot{v} - \rho_1 \ddot{w}_{,y} + \rho_0^{21} \ddot{v}_1 + \rho_0^{41} \ddot{u}_1,\\
&M^c_{x,xx} + M^c_{y,yy} + 2M^c_{xy,xy} = \rho_0 \ddot{w} - \rho_2(\ddot{w}_{,xx} + \ddot{w}_{,yy}) + \rho_1(\ddot{u}_{,x} + \ddot{v}_{,y}) + \rho_1^{11} \ddot{u}_{1,x} + \rho_1^{21} \ddot{v}_{1,y} + \rho_1^{31} \ddot{v}_{1,x} + \rho_1^{41} \ddot{u}_{1,y},\\
&M^a_{x,x} + M^a_{xy,y} - Q^a_x = \rho_0^{11} \ddot{u} - \rho_1^{11} \ddot{w}_{,x} + \rho_0^{12} \ddot{u}_1 + \rho_0^{41} \ddot{v} - \rho_1^{41} \ddot{w}_{,y} + \rho_0^{42} \ddot{u}_1 + (\rho_0^{1131} + \rho_0^{2141}) \ddot{v}_1,\\
&M^a_{y,y} + M^a_{yx,x} - Q^a_y = \rho_0^{21} \ddot{v} - \rho_1^{21} \ddot{w}_{,y} + \rho_0^{22} \ddot{v}_1 + \rho_0^{31} \ddot{u} - \rho_1^{31} \ddot{w}_{,x} + \rho_0^{32} \ddot{v}_1 + (\rho_0^{1131} + \rho_0^{2141}) \ddot{u}_1.
\end{aligned}
\tag{8}
$$

The inertia terms that appear in the right hand sides of these equations are defined as follows:

$$
\rho_k = \int_{-h/2}^{h/2} \rho z^k \, \mathrm{d}z; \quad \rho_k^{lmno} = \int_{-h/2}^{h/2} \rho \Phi_l^m \Phi_n^o z^k \, \mathrm{d}z; \quad \rho_k^{lm} = \int_{-h/2}^{h/2} \rho \Phi_l^m z^k \, \mathrm{d}z, \tag{9}
$$

where ρ denotes the material density of the elastic plate considered. It should be further noted that, unlike the afore-mentioned vectorial approach (Soldatos, 1993), Hamilton's principle also yields all possible sets of variationally consistent boundary conditions that can be applied on a plate edge. For the case of a rectangular flat plate, like the one shown in Fig. 1, the following quantities must be prescribed along the edges:

$$
\begin{aligned}
&\text{at } x = 0,\ L_x: && \text{at } y = 0,\ L_y:\\
&\quad \text{either } u \text{ or } N_x, && \quad \text{either } v \text{ or } N_y,\\
&\quad \text{either } v \text{ or } N_{xy}, && \quad \text{either } u \text{ or } N_{xy},\\
&\quad \text{either } w \text{ or } (M_{x,x} + 2M_{xy,y} - \rho_1 \ddot{u} && \quad \text{either } w \text{ or } (M_{y,y} + 2M_{xy,x} - \rho_1 \ddot{v}\\
&\qquad\qquad + \rho_2 \ddot{w}_{,x} - \rho_1^{11} \ddot{u}_1 - \rho_1^{31} \ddot{v}_1), && \qquad\qquad + \rho_2 \ddot{w}_{,y} - \rho_1^{41} \ddot{u}_1 - \rho_1^{21} \ddot{v}_1),\\
&\quad \text{either } u_1 \text{ or } M^a_x, && \quad \text{either } v_1 \text{ or } M^a_y,\\
&\quad \text{either } v_1 \text{ or } M^a_{yx}, && \quad \text{either } u_1 \text{ or } M^a_{xy},\\
&\quad \text{either } w_{,x} \text{ or } M_x. && \quad \text{either } w_{,y} \text{ or } M_y.
\end{aligned}
\tag{10}
$$

3. Consideration of interlaminar stress continuity in angle-ply laminate plates

Consider next the case of a rectangular elastic plate made of an arbitrary number, L, of linearly elastic monoclinic layers. Accordingly, the generalised Hooke's law within the kth layer of such a laminate (starting counting from the bottom layer) is given as follows ($k = 1, 2, \ldots, L$):

$$
\begin{bmatrix} \sigma_x^{(k)} \\ \sigma_y^{(k)} \\ \tau_{xy}^{(k)} \end{bmatrix} = \begin{bmatrix} Q_{11}^{(k)} & Q_{12}^{(k)} & Q_{16}^{(k)} \\ Q_{12}^{(k)} & Q_{22}^{(k)} & Q_{26}^{(k)} \\ Q_{16}^{(k)} & Q_{26}^{(k)} & Q_{66}^{(k)} \end{bmatrix} \begin{bmatrix} \varepsilon_x \\ \varepsilon_y \\ \gamma_{xy} \end{bmatrix}, \tag{11a}
$$

$$
\begin{bmatrix} \tau_{yz}^{(k)} \\ \tau_{xz}^{(k)} \end{bmatrix} = \begin{bmatrix} Q_{44}^{(k)} & Q_{45}^{(k)} \\ Q_{45}^{(k)} & Q_{55}^{(k)} \end{bmatrix} \begin{bmatrix} \gamma_{yz} \\ \gamma_{xz} \end{bmatrix}, \tag{11b}
$$

where Q's are the well-known reduced elastic stiffnesses (Jones, 1975; Whitney, 1987).

Introduction of these equations into Eq. (7) yields then the force and moment resultants in terms of the five degrees of freedom and their derivatives, as follows:

$$
\begin{pmatrix} N_x^c \\ N_y^c \\ N_{xy}^c \\ M_x^c \\ M_y^c \\ M_{xy}^c \\ M_x^a \\ M_y^a \\ M_{xy}^a \\ M_{yx}^a \end{pmatrix}
=
\begin{bmatrix}
A_{11} & A_{12} & A_{16} & B_{11} & B_{12} & B_{16} & B_{111}+B_{164} & B_{122}+B_{163} & B_{124}+B_{161} & B_{162}+B_{113} \\
 & A_{22} & A_{26} & B_{12} & B_{22} & B_{26} & B_{121}+B_{264} & B_{222}+B_{263} & B_{224}+B_{261} & B_{262}+B_{123} \\
 & & A_{66} & B_{16} & B_{26} & B_{66} & B_{161}+B_{664} & B_{262}+B_{663} & B_{264}+B_{661} & B_{163}+B_{662} \\
 & & & D_{11} & D_{12} & D_{16} & D_{111}+D_{164} & D_{122}+D_{163} & D_{124}+D_{161} & D_{113}+D_{162} \\
 & & & & D_{22} & D_{26} & D_{121}+D_{264} & D_{222}+D_{263} & D_{224}+D_{261} & D_{123}+D_{262} \\
 & & & & & D_{66} & D_{161}+D_{664} & D_{262}+D_{663} & D_{264}+D_{661} & D_{163}+D_{662} \\
 & & \text{sym} & & & & \begin{pmatrix} D_{1111}+D_{6644} \\ +2D_{1614} \end{pmatrix} & \begin{pmatrix} D_{1221}+D_{2624} \\ +D_{1631}+D_{6634} \end{pmatrix} & \begin{pmatrix} D_{1611}+D_{2644} \\ +D_{1241}+D_{6614} \end{pmatrix} & \begin{pmatrix} D_{1621}+D_{6624} \\ +D_{1131}+D_{1634} \end{pmatrix} \\
 & & & & & & & \begin{pmatrix} D_{2222}+D_{6633} \\ +2D_{2623} \end{pmatrix} & \begin{pmatrix} D_{2242}+D_{2612} \\ +D_{2643}+D_{6613} \end{pmatrix} & \begin{pmatrix} D_{1232}+D_{2622} \\ +D_{1633}+D_{6623} \end{pmatrix} \\
 & & & & & & & & \begin{pmatrix} D_{2244}+D_{6611} \\ +2D_{2614} \end{pmatrix} & \begin{pmatrix} D_{1234}+D_{2624} \\ +D_{1631}+D_{6621} \end{pmatrix} \\
 & & & & & & & & & \begin{pmatrix} D_{1133}+D_{6622} \\ +2D_{1632} \end{pmatrix}
\end{bmatrix}
\times
\begin{bmatrix} u_{,x} \\ v_{,y} \\ u_{,y}+v_{,x} \\ -w_{,xx} \\ -w_{,yy} \\ -2w_{,xy} \\ u_{1,x} \\ v_{1,y} \\ u_{1,y} \\ v_{1,x} \end{bmatrix}, \tag{12a}
$$

$$
\begin{pmatrix} Q_y^a \\ Q_x^a \end{pmatrix}
=
\begin{bmatrix} (A_{4422}+2A_{4532}+A_{5533}) & (A_{4422}+A_{4512}+A_{4543}+A_{5513}) \\ \text{sym} & (A_{4444}+2A_{4514}+A_{5511}) \end{bmatrix}
\begin{bmatrix} v_1 \\ u_1 \end{bmatrix}, \tag{12b}
$$

where the appearing extensional, coupling and bending rigidities are defined according to:

$$
\begin{aligned}
A_{ij} &= \int_{-h/2}^{h/2} Q_{ij}^{(k)}\,\mathrm{d}z, \quad B_{ij} = \int_{-h/2}^{h/2} Q_{ij}^{(k)} z\,\mathrm{d}z, \quad B_{ijp} = \int_{-h/2}^{h/2} Q_{ij}^{(k)} \Phi_p\,\mathrm{d}z, \\
D_{ij} &= \int_{-h/2}^{h/2} Q_{ij}^{(k)} z^2\,\mathrm{d}z, \quad D_{ijp} = \int_{-h/2}^{h/2} Q_{ij}^{(k)} \Phi_p z\,\mathrm{d}z, \quad D_{ijpm} = \int_{-h/2}^{h/2} Q_{ij}^{(k)} \Phi_p \Phi_m\,\mathrm{d}z, \\
A_{ijpm} &= \int_{-h/2}^{h/2} Q_{ij}^{(k)} \Phi'_p \Phi'_m\,\mathrm{d}z.
\end{aligned} \tag{13}
$$

With the use of the 2D constitutive Eqs. (12a) and (12b), the equations of motion (8) can be converted into a set of five simultaneous differential equations for the same number of main unknowns. The number of the boundary conditions (10) suggests that this will be a 12-order set of partial differential equations, which may be solved simultaneously when a particular set of boundary conditions is specified at each edge of the plate. It should be noted however that use of Eqs. (12a) and (12b) can be made only after the four global shape functions involved in the model are specified and, hence, the integrations denoted in Eq. (13) are performed.

The purpose of this section is to outline a process of making these shape functions capable to satisfy continuity of displacements and transverse shear stresses at the interfaces of a laminate, the layers of which obey the constitutive Eqs. (11a) and (11b). The process will be outlined for the case of symmetric angle-ply laminates only and may therefore be considered as a generalisation of the corresponding process outlined in Timarci and Soldatos (1995) for symmetric lay-ups. As far as antisymmetric angle-ply laminates are concerned, it may further be considered as a generalisation of the process outlined in Messina and Soldatos (1999a), for corresponding cross-ply lay-ups. Although some of the numerical results shown in Section 5 reveal that this later version of the process is also available to the authors, it will not be presented here for the sake of brevity.

Hence, consider only the case a laminated plate composed of an odd number (say $L = 2N + 1$) of linearly elastic monoclinic layers which are perfectly bonded together. As shown in Fig. 1, denote further with a superscript "(0)" all quantities referring to the middle layer of the plate and denote further by z_k the transverse co-ordinate of the material interface between the $(k \pm 1)$th and the kth layer ($k = \pm 1, \pm 2, \ldots, \pm N$). Consider next the kth layer ($k = 0, \pm 1, \pm 2, \ldots, \pm N$) as an independent plate and, in accordance with the global displacement approximation (2), assume that its displacement field is approximated as follows:

$$\begin{aligned} U^{(k)} &= u_0^{(k)} - zw_{,x} + \varphi_1^{(k)}(z)u_1^{(k)} + \varphi_3^{(k)}(z)v_1^{(k)}, \\ V^{(k)} &= v_0^{(k)} - zw_{,y} + \varphi_2^{(k)}(z)v_1^{(k)} + \varphi_4^{(k)}(z)u_1^{(k)}, \\ W^{(k)} &= w^{(k)} = w. \end{aligned} \tag{14}$$

In accordance with the constitutive equations the last two terms of Eq. (3) and Eq. (11b), denote also that transverse shear stresses and strains in the kth layer are related as follows:

$$\begin{bmatrix} \tau_{yz}^{(k)} \\ \tau_{xz}^{(k)} \end{bmatrix} = \begin{bmatrix} (Q_{44}^{(k)}\varphi_2'^{(k)} + Q_{45}^{(k)}\varphi_3'^{(k)}) & (Q_{44}^{(k)}\varphi_4'^{(k)} + Q_{45}^{(k)}\varphi_1'^{(k)}) \\ (Q_{45}^{(k)}\varphi_2'^{(k)} + Q_{55}^{(k)}\varphi_3'^{(k)}) & (Q_{45}^{(k)}\varphi_4'^{(k)} + Q_{55}^{(k)}\varphi_1'^{(k)}) \end{bmatrix} \begin{bmatrix} v_1^{(k)} \\ u_1^{(k)} \end{bmatrix}. \tag{15}$$

Then, upon requiring continuity of these interlaminar stresses at z_k, and following essentially the procedure outlined in Timarci and Soldatos (1995) for cross-ply laminates, one obtains the relationship,

$$\begin{bmatrix} v_1^{(k)} \\ u_1^{(k)} \end{bmatrix} = \underbrace{\begin{bmatrix} A_{11}^{(k)} & A_{12}^{(k)} \\ A_{21}^{(k)} & A_{22}^{(k)} \end{bmatrix}}_{[A^{(k)}]} \begin{bmatrix} v_1^{(0)} \\ u_1^{(0)} \end{bmatrix}. \tag{16}$$

The elements of the appearing 2×2 matrices $[A^{(k)}]$ are obtained in accordance with the following recurrence formula ($k = \pm 1, \pm 2, \ldots, \pm N$):

$$\left[A^{(k)}\right] = \begin{pmatrix} \begin{bmatrix} (Q_{44}^{(k)}\varphi_2'^{(k)}(z_k) + Q_{45}^{(k)}\varphi_3'^{(k)}(z_k)) & (Q_{44}^{(k)}\varphi_4'^{(k)}(z_k) + Q_{45}^{(k)}\varphi_1'^{(k)}(z_k)) \\ (Q_{45}^{(k)}\varphi_2'^{(k)}(z_k) + Q_{55}^{(k)}\varphi_3'^{(k)}(z_k)) & (Q_{45}^{(k)}\varphi_4'^{(k)}(z_k) + Q_{55}^{(k)}\varphi_1'^{(k)}(z_k)) \end{bmatrix}^{-1} \\ \begin{bmatrix} (Q_{44}^{(k\mp1)}\varphi_2'^{(k\mp1)}(z_k) + Q_{45}^{(k\mp1)}\varphi_3'^{(k\mp1)}(z_k)) & (Q_{44}^{(k\mp1)}\varphi_4'^{(k\mp1)}(z_k) + Q_{45}^{(k\mp1)}\varphi_1'^{(k\mp1)}(z_k)) \\ (Q_{45}^{(k\mp1)}\varphi_2'^{(k\mp1)}(z_k) + Q_{55}^{(k\mp1)}\varphi_3'^{(k\mp1)}(z_k)) & (Q_{45}^{(k\mp1)}\varphi_4'^{(k\mp1)}(z_k) + Q_{55}^{(k\mp1)}\varphi_1'^{(k\mp1)}(z_k)) \end{bmatrix} \end{pmatrix} \left[A^{(k\mp1)}\right], \tag{17}$$

where, as Eq. (16) itself reveals, $[A^{(0)}]$ is a 2×2 identity matrix. It should be noted that the upper and the lower signs appearing in on the right hand side of Eq. (17) are associated with positive and negative values of k, respectively.

Upon inserting expressions (16) into Eq. (14) and upon, then, requiring continuity of the displacement components on the z_k material interface, one obtains further,

$$\begin{aligned} u_0^{(k)} &= u_0^{(0)} + B_1^{(k)}u_1^{(0)} + B_3^{(k)}v_1^{(0)}, \\ v_0^{(k)} &= v_0^{(0)} + B_2^{(k)}v_1^{(0)} + B_4^{(k)}u_1^{(0)}, \end{aligned} \tag{18}$$

where,

$$\begin{aligned} B_1^{(k)} &= B_1^{(k\mp1)} + \left[(\varphi_1^{(k\mp1)}(z_k)A_{22}^{(k\mp1)} + \varphi_3^{(k\mp1)}(z_k)A_{12}^{(k\mp1)}) - (\varphi_1^{(k)}(z_k)A_{22}^{(k)} + \varphi_3^{(k)}(z_k)A_{12}^{(k)})\right], \quad B_1^{(0)} = 0, \\ B_3^{(k)} &= B_3^{(k\mp1)} + \left[(\varphi_1^{(k\mp1)}(z_k)A_{21}^{(k\mp1)} + \varphi_3^{(k\mp1)}(z_k)A_{11}^{(k\mp1)}) - (\varphi_1^{(k)}(z_k)A_{21}^{(k)} + \varphi_3^{(k)}(z_k)A_{11}^{(k)})\right], \quad B_3^{(0)} = 0, \\ B_2^{(k)} &= B_2^{(k\mp1)} + \left[(\varphi_2^{(k\mp1)}(z_k)A_{11}^{(k\mp1)} + \varphi_4^{(k\mp1)}(z_k)A_{21}^{(k\mp1)}) - (\varphi_2^{(k)}(z_k)A_{11}^{(k)} + \varphi_4^{(k)}(z_k)A_{21}^{(k)})\right], \quad B_2^{(0)} = 0, \\ B_4^{(k)} &= B_4^{(k\mp1)} + \left[(\varphi_4^{(k\mp1)}(z_k)A_{22}^{(k\mp1)} + \varphi_2^{(k\mp1)}(z_k)A_{12}^{(k\mp1)}) - (\varphi_4^{(k)}(z_k)A_{22}^{(k)} + \varphi_2^{(k)}(z_k)A_{12}^{(k)})\right], \quad B_4^{(0)} = 0. \end{aligned} \tag{19}$$

Hence, with the use of expressions (16) and (18), the displacement field (14) is finally obtained in the following form:

$$\begin{aligned} U^{(k)} &= u_0^{(0)} - zw_{,x} + \Phi_1^{(k)}(z)u_1^{(0)} + \Phi_3^{(k)}(z)v_1^{(0)}, \\ V^{(k)} &= v_0^{(0)} - zw_{,y} + \Phi_2^{(k)}(z)v_1^{(0)} + \Phi_4^{(k)}(z)u_1^{(0)}, \\ W^{(k)} &= w^{(0)} = w, \end{aligned} \tag{20}$$

where,

$$\begin{aligned} \Phi_1^{(k)}(z) &= B_1^{(k)} + \varphi_1^{(k)}(z)A_{22}^{(k)} + \varphi_3^{(k)}(z)A_{12}^{(k)}, \\ \Phi_3^{(k)}(z) &= B_3^{(k)} + \varphi_1^{(k)}(z)A_{21}^{(k)} + \varphi_3^{(k)}(z)A_{11}^{(k)}, \\ \Phi_2^{(k)}(z) &= B_2^{(k)} + \varphi_2^{(k)}(z)A_{11}^{(k)} + \varphi_4^{(k)}(z)A_{21}^{(k)}, \\ \Phi_4^{(k)}(z) &= B_4^{(k)} + \varphi_2^{(k)}(z)A_{12}^{(k)} + \varphi_4^{(k)}(z)A_{22}^{(k)}. \end{aligned} \tag{21}$$

A comparison of the displacement field (20) with the displacement approximation (2) makes it clear that this is essentially a global displacement approximation suitable for use in association with the five degrees of freedom shell theory developed in the preceding section. In more detail, the five unknown displacement functions, $u_0^{(0)}$, $v_0^{(0)}$, $w_0^{(0)}$, $u_1^{(0)}$ and $v_1^{(0)}$, of the middle layer of the plate are now the five degrees of freedom of the model. Most importantly, for any set of a posteriori specified shape functions, $\varphi_1^{(k)}(z)$, $\varphi_2^{(k)}(z)$, $\varphi_3^{(k)}(z)$ and $\varphi_4^{(k)}(z)$ ($k = 0, \pm1, \pm2, \ldots, \pm N$), the global displacement approximation (20) is capable of satisfying the interlaminar continuity conditions of both displacements and transverse shear stresses. It should be

noted in this respect that the complicated looking form of the recurrence formulas (17) and (19) do not add any additional difficulties in the computational effort involved during a particular application of the present shear deformable model. This is because, if necessary, the quantities defined in Eqs. (9) and (13) can always be evaluated numerically by means of a standard numerical routine. The present angle-ply laminated plate theory preserves therefore all the valuable features of a corresponding layer-wise model but, making use of only five main unknown quantities, it keeps the computational effort required independent of the number of layers involved.

4. Cylindrical bending modes of angle-ply laminated plates

An effective way to test the reliability of a 2D model, like the one developed in the preceding sections, is by performing numerical comparisons with corresponding results of an exact 3D solution, if available, of a relatively simple elasticity problem. As far as angle-ply laminated plates are concerned, the authors are however unaware of such a simple, dynamic, 3D elasticity solution. It was therefore decided that such a reasonably simple testing situation could be reached only after an appropriate extension of the corresponding static, cylindrical bending solution (Pagano, 1970) towards the free vibrations of angle-ply laminated plates. This dynamic extension of Pagano (1970) elasticity solution is next detailed in this section and is followed by the corresponding solution obtained on the basis of the present 2D model. The cylindrical bending modes of angle-ply laminated plates thus obtained can alternatively be considered as the axisymmetric free vibration modes of an angle-ply laminated circular cylindrical shell having an infinite middle-surface radius (Soldatos and Ye, 1995; Timarci and Soldatos, 2000).

4.1. Exact elasticity solution

Consider the elastic plate shown in Fig. 2, which has a constant thickness, h a constant axial length, L_x, but has an infinite width ($L_y = \infty$). Like in Fig. 1, the in-plane and normal to the middle-surface coordinate length parameters are denoted with x, y and z, respectively, whereas U, V and W represent the

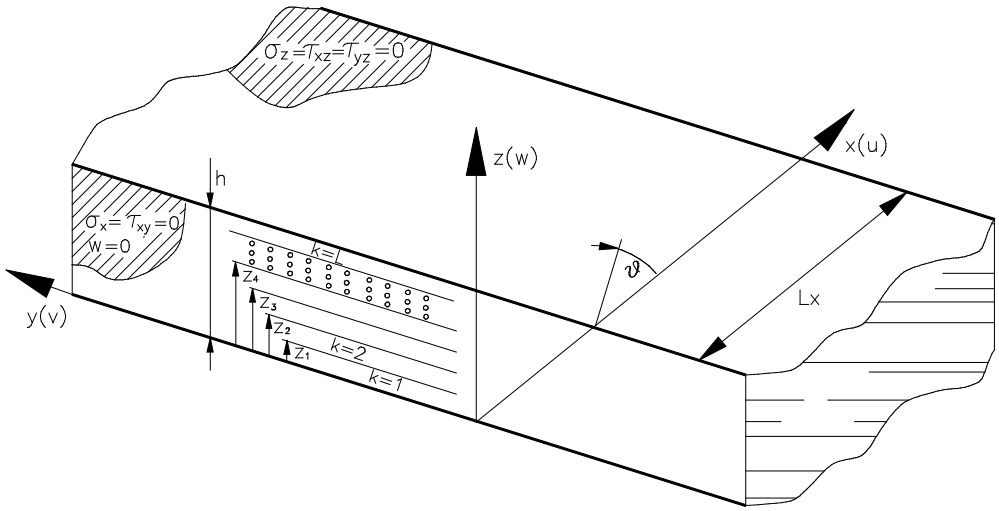

Fig. 2. Notation used for the 3D modelling of symmetric or antisymmetric laminated plates.

corresponding displacement components. Moreover, the plate is assumed as being made of an arbitrary number, L, of linearly elastic monoclinic layers. Accordingly, the principle material axis in each layer is assumed to form an angle θ with respect to the x-axis of the adopted Cartesian co-ordinate system. Hence, the main difference on the present nomenclature from that adopted in Fig. 1 is that the origin of the Cartesian co-ordinate system shown in Fig. 2 is located at the bottom of lateral plane of the plate.

The cylindrical bending modes of the infinite plate shown in Fig. 2 are the ones that are independent of the y co-ordinate, namely the ones in which all the plate cross-sections vibrate freely in an identical pattern. Accordingly, the plate displacement components have the following form:

$$\begin{aligned} U(x,y,z;t) &= U(x,z;t),\\ V(x,y,z;t) &= V(x,z;t),\\ W(x,y,z;t) &= W(x,z;t), \end{aligned} \tag{22}$$

which does not depend on the y co-ordinate parameter. Hence, in each one of the monoclinic layers considered, the dynamic version of the Navier elasticity equations takes the following form:

$$\begin{aligned} &C_{11}U_{,xx} + C_{13}W_{,zx} + C_{16}V_{,xx} + C_{45}V_{,zz} + C_{55}W_{,xz} + C_{55}U_{,zz} = \rho\ddot{U},\\ &C_{16}U_{,xx} + C_{36}W_{,zx} + C_{66}V_{,xx} + C_{44}V_{,zz} + C_{45}W_{,xz} + C_{45}U_{,zz} = \rho\ddot{V},\\ &C_{45}V_{,zx} + C_{55}W_{,xx} + C_{55}U_{,zx} + C_{13}U_{,xz} + C_{33}W_{,zz} + C_{36}V_{,xz} = \rho\ddot{W}, \end{aligned} \tag{23}$$

where C's are the corresponding elastic constants (Pagano, 1970; Jones, 1975; Whitney, 1987).

Eq. (23) are susceptible of an exact solution, provided that both plate edges, $x = 0$ and $x = L_x$, are subjected to the following set of simply supported boundary conditions:

$$\begin{aligned} &w = 0,\\ &\sigma_x = \tau_{xy} = 0. \end{aligned} \tag{24}$$

As can easily be verified, these boundary conditions are exactly satisfied by a displacement field of the form,

$$\begin{aligned} U(x,z;t) &= u(z)\cos(n\pi x/L_x)\cos(\omega t),\\ V(x,z;t) &= v(z)\cos(n\pi x/L_x)\cos(\omega t),\\ W(x,z;t) &= w(z)\sin(n\pi x/L_x)\cos(\omega t), \end{aligned} \tag{25}$$

in which ω represents an unknown natural frequency of vibration and n is a positive integer that represents the wave number of the particular mode along the x direction. Moreover, with the use of the displacement field (25), the set of the partial differential equations (23) is converted into a corresponding sixth-order set of simultaneous homogeneous ordinary differential equations, the matrix form of which is as follows:

$$\begin{bmatrix} (-C_{11}m^2 + D^2C_{55} + \rho\omega^2) & (-C_{16}m^2 + D^2C_{45}) & mD(C_{13} + C_{55}) \\ (-C_{16}m^2 + D^2C_{45}) & (-C_{66}m^2 + D^2C_{44} + \rho\omega^2) & mD(C_{36} + C_{45}) \\ -mD(C_{13} + C_{55}) & -mD(C_{36} + C_{45}) & (-C_{55}m^2 + D^2C_{33} + \rho\omega^2) \end{bmatrix} \begin{bmatrix} u(z) \\ v(z) \\ w(z) \end{bmatrix} = \begin{bmatrix} 0 \\ 0 \\ 0 \end{bmatrix}, \tag{26}$$

with $m = n\pi/L_x$ and $D = \mathrm{d}/\mathrm{d}z$. Eq. (26) can equivalently be expressed into the following form of six first-order simultaneous ordinary differential equations:

$$\{F(z)\}' = [G]\{F(z)\}, \qquad \{F(z)\}^T = \{u, v, w, u', v', w'\}, \tag{27}$$

where, the elements of the 6×6 matrix $[G]$ are given in Appendix A.

In the case of a homogeneous monoclinic plate, the general solution of Eq. (27) can be expressed in the form,

$$\{F(z)\} = [P(z)]\{F(0)\}, \quad 0 \leqslant z \leqslant h, \tag{28}$$

where, $\{F(0)\}$ denotes the value of the vector $\{F\}$ at the bottom lateral plane of the plate. For a given value of z, the elements of the exponential matrix $[P(z)] = \exp[(z)G]$ can be evaluated numerically. By connecting the solution (28) with the zero traction boundary conditions applied on the plate lateral planes, one obtains the final 6×6 algebraic eigenvalue problem whose solution will provide the natural frequencies and mode shapes sought. In the present case of a plate involving L monoclinic layers, the set of solutions of the form (28) obtained for each layer have also to be connected through appropriate continuity conditions. A corresponding efficient formulation is detailed in Soldatos and Ye (1995) and, for the sake of brevity, will not be repeated here. In Soldatos and Ye (1995), this formulation was outlined for 3D axisymmetric vibrations of a circular cylinder with monoclinic layers. In the limiting case, however, in which the radius of curvature of the cylinder approaches infinity, this will be reduced to the corresponding formulation that is appropriate for the plate problem considered in this section. As detailed in Soldatos and Ye (1995) (see also Fan and Ye (1990)), this yields the solution of the vibration problem considered by making use of 6×6 matrices only, regardless of the total number, L, of the monoclinic layers involved.

4.2. Solution based on the present two-dimensional model

As far as the present 2D plate model is concerned, the simply supported edge boundary conditions that correspond to 3D boundary conditions (24) are as follows (at $x = 0$ and $x = L_x$):

$$\begin{aligned} &w = 0, \\ &N_x^c = N_{xy}^c = 0, \\ &M_x^c = M_x^a = M_{yx}^a = 0. \end{aligned} \tag{29}$$

In the context outlined in the preceding subsection, the following displacement field:

$$\begin{aligned} &(u, v, u_1, v_1) = A^{(u,v,u_1,v_1)} \cos\left(\tfrac{n\pi x}{L_x}\right) \cos(\omega t), \\ &w = A^{(w)} \sin\left(\tfrac{n\pi x}{L_x}\right) \cos(\omega t), \end{aligned} \tag{30}$$

satisfies exactly the boundary conditions. Hence upon specialising the Navier-type form of Eq. (8) in accordance with the present vibration assumptions and, then, making use of the displacement model (30), one obtains the following eigenvalue problem:

$$(\mathbf{K} - \omega^2 \mathbf{M})\mathbf{X} = \mathbf{0}, \quad \mathbf{X} = (A^{(u)},\ A^{(v)},\ A^{(w)},\ A^{(u_1)},\ A^{(v_1)})^T, \tag{31}$$

the stiffness and mass matrices of which are as follows (for $m \neq 0$):

$$\mathbf{K} = m^2 \begin{bmatrix} A_{11} & A_{16} & -mB_{11} & B_{111} + \delta B_{164} & B_{162} + \delta B_{113} \\ & A_{66} & -mB_{16} & B_{161} + \delta B_{664} & \delta B_{163} + B_{662} \\ & & m^2 D_{11} & -m(D_{111} + \delta D_{164}) & -m(D_{162} + \delta D_{113}) \\ & \text{sym} & & \begin{pmatrix} D_{1111} + 2\delta D_{1614} + \delta D_{6644} \\ +(\delta A_{4444} + 2\delta A_{4514} + A_{5511})/m^2 \end{pmatrix} & \begin{pmatrix} D_{1612} + \delta D_{6624} + \delta D_{1131} + \delta D_{1634} \\ +(A_{4521} + \delta A_{5531} + \delta A_{4424} + \delta A_{4534})/m^2 \end{pmatrix} \\ & & & & \begin{pmatrix} \delta D_{1133} + 2\delta D_{1632} + D_{6622} \\ +(A_{4422} + 2\delta A_{4532} + \delta A_{5533})/m^2 \end{pmatrix} \end{bmatrix}, \tag{32}$$

$$\mathbf{M} = \begin{bmatrix} \rho_0 & 0 & -m\rho_1 & \rho_0^{11} & \delta\rho_0^{31} \\ & \rho_0 & 0 & \delta\rho_0^{41} & \rho_0^{21} \\ & & \rho_0 + m^2\rho_2 & -m\rho_1^{11} & -m\delta\rho_1^{31} \\ & \text{sym} & & \rho_0^{12} + \delta\rho_0^{42} & \delta\left(\rho_0^{1131} + \rho_0^{2141}\right) \\ & & & & \rho_0^{22} + \delta\rho_0^{32} \end{bmatrix}. \tag{33}$$

Here $m = \pi n/L_x$ whereas the appearing δ-index can be assigned the values 0 and 1. A zero value of δ-operator is associated with choices of the global shape functions that, as they appear in Eq. (2), violate the continuity of the interlaminar shear stresses. The value $\delta = 1$ is associated with choices of the local shape functions that yield continuous interlaminar shear stresses, in the sense described in Section 3.

5. A numerical test

The efficiency of the present, general, 2D model can be tested only after particular forms are assigned to the shape functions involved. In the present study, the $\delta = 0$ value of the δ-index that appears in Eqs. (32) and (33) is only associated with the choice,

$$\begin{aligned} &\Phi_1 = \Phi_2 = z(1 - 4z^2/3h^2), \\ &\Phi_3 = \Phi_4 = 0, \end{aligned} \tag{34}$$

which results into a conventional PSDPT that yields discontinuous interlaminar stresses (PSDPT_{ds}). In this connection, the $\delta = 1$ value is associated with the choice,

$$\varphi_1^{(k)} = -\varphi_3^{(k)} = \varphi_2^{(k)} = \varphi_4^{(k)} = z(1 - 4z^2/3h^2), \tag{35}$$

which results into an advanced PSDPT that satisfies continuity at interlaminar stresses (PSDPT_{cs}). It is denoted however that, despite their difference, both the PSDPT_{ds} and the PSDPT_{cs} satisfy the zero shear traction boundary conditions imposed on the lateral planes of the plate. Hence, none of these theories needs the use of a shear correction factor in the sense requited by their uniform shear deformable counterparts.

Under these considerations, the numerical results presented in this section have a twofold objective. Firstly, to test the effectiveness of the 2D model introduced in Sections 2 and 3 by comparing its predictions against corresponding 3D elasticity results obtained for cylindrical bending vibration modes. Afterwards, to investigate the reasons that possibly introduce discrepancies between corresponding natural frequencies obtained on the basis of the PSDPT_{ds} and PSDPT_{cs} models. To this end the eigenfunctions of both of these 2D models are plotted and carefully examined in comparisons with their relevant 3D elasticity counterparts.

Unless it is not differently specified, the following material properties are used for most of the numerical tests:

$$E_1 = 25E_2 = 25E_3; \quad G_{12} = G_{13} = 0.5E_2; \quad G_{23} = 0.2E_2; \quad v_{12} = v_{13} = v_{23} = 0.25 \tag{36}$$

with the relevant geometric parameters indicated in each one of the table headings. Finally, the dimensionless frequency parameter employed is defined as follows:

$$\omega^* = \omega h\sqrt{\frac{\rho}{G_{12}}}. \tag{37}$$

Tables 1 and 2 compare natural frequencies of two-layered antisymmetric and three-layered symmetric laminates, respectively, that correspond to bending vibrational modes, namely frequencies whose w-mode-shapes component is dominant with respect to its in-plane counterparts (u, v). The comparison is presented

Table 1
Lowest frequency parameter, ω^*, as a function of the lamination angle (pattern: $[+\theta/-\theta]$; $L_x/h = 10$; $n = 1$)

θ (°)	3D	PSDPT$_{cs}$	PSDPT$_{ds}$
0	0.16489	0.16484	0.16484
15	0.11541	0.11615	0.11583
30	0.088013	0.089233	0.088461
45	0.065634	0.066363	0.065839
60	0.048226	0.048374	0.048256
75	0.040409	0.040399	0.040421
90	0.039250	0.039235	0.039235

Table 2
Lowest frequency parameter, ω^*, as a function of the lamination angle (pattern: $[+\theta/-\theta/+\theta]$; $L_x/h = 10$; $n = 1$)

θ (°)	3D	PSDPT$_{cs}$	PSDPT$_{ds}$
0	0.16489	0.16484	0.16484
15	0.15232	0.15231	0.15330
30	0.12396	0.12401	0.12636
45	0.091114	0.091150	0.092959
60	0.059879	0.059874	0.060344
75	0.041722	0.041706	0.041754
90	0.039250	0.039235	0.039235

by using different lamination angles. Both Tables 1 and 2 reveal an excellent agreement between the 2D results and their exact 3D elasticity counterparts. However, it is evident that the PSDPT$_{cs}$ model yields frequencies that are closer to the exact elasticity ones in the case of the symmetric stacking pattern (Table 2), for which there in no bending–extension coupling due to lamination (see, also Messina and Soldatos (1999a)). Contrary to this, the PSDPT$_{ds}$ model is more accurate in case of the two-layered antisymmetric laminates (Table 1) for which that bending–stretching coupling has a profound effect. Moreover, between the two frequencies predicted by using PSDPT$_{cs}$ and PSDPT$_{ds}$, it is always the lowest one that is the nearer to the corresponding exact 3D elasticity prediction. These conclusions are reinforced from the results presented in Table 3, which considers $[45°/-45°]$ and $[45°/-45°/45°]$ plates and compares corresponding lowest frequency parameters obtained by increasing the wave number. These comparisons make again evident that, in general, the PSDPT$_{cs}$ (PSDPT$_{ds}$) model behaves better in the case of symmetric (antisymmetric) laminates. An exception to this rule appears to be when $n = 4$ for symmetric laminates, where

Table 3
Lowest frequency parameter, ω^*, as a function of the wave number ($h/L_x = 0.1$)

	n	3D	PSDPT$_{cs}$	PSDPT$_{ds}$
$[45°/-45°]$	1	0.065634	0.066363	0.065839
	2	0.23545	0.24492	0.23808
	3	0.46217	0.49924	0.47222
	4	0.71412	0.80426	0.73782
$[45°/-45°/45°]$	1	0.091114	0.091150	0.092959
	2	0.27537	0.27637	0.28489
	3	0.48913	0.49535	0.50487
	4	0.72074	0.74126	0.73951

Table 4
Lowest frequency parameter, ω^*, as a function of the ratio G_{23}/E_2 ($L_x/h = 10; n = 1$)

G_{23}/E_2	$[30°/-30°]$			$[30°/-30°]_6$		
	$PSDPT_{cs}$	$PSDPT_{ds}$	$\Delta\%$	$PSDPT_{cs}$	$PSDPT_{ds}$	$\Delta\%$
0.50	0.089091	0.089091	0.00	0.13444	0.13444	0.00
0.45	0.089110	0.088999	0.12	0.13403	0.13406	−0.02
0.40	0.089131	0.088902	0.26	0.13352	0.13367	−0.11
0.35	0.089154	0.088800	0.40	0.13288	0.13326	−0.29
0.30	0.089180	0.088693	0.55	0.13203	0.13283	−0.61
0.25	0.089208	0.088580	0.70	0.13088	0.13239	−1.15
0.20	0.089233	0.088461	0.87	0.12920	0.13192	−2.11

Table 5
Lowest frequency parameter, ω^*, as a function of the ratio E_2/E_1 ($L_x/h = 10; n = 1$)

E_1/E_2	$[30°/-30°]$			$[30°/-30°]_6$		
	$PSDPT_{cs}$	$PSDPT_{ds}$	$\Delta\%$	$PSDPT_{cs}$	$PSDPT_{ds}$	$\Delta\%$
1	0.042172	0.042267	−0.23	0.042236	0.042326	−0.21
5	0.059826	0.059879	−0.09	0.070376	0.070803	−0.61
10	0.069467	0.069353	0.16	0.091921	0.092884	−1.05
20	0.083396	0.082861	0.64	0.11939	0.12153	−1.79
25	0.089233	0.088461	0.87	0.12920	0.13192	−2.11
30	0.094597	0.093575	1.08	0.13743	0.14071	−2.39
40	0.10426	0.10270	1.50	0.15058	0.15491	−2.88

the $PSDPT_{ds}$ prediction is better than that of the $PSDPT_{cs}$ model. It is however again observed that, between two different frequency predictions, the lowest one is always nearer to its corresponding exact 3D elasticity counterpart.

Tables 4 and 5 compare further corresponding lowest natural frequencies of plates having 2 and 12 layers, respectively, in an antisymmetric stacking pattern with a lamination angle $\theta = 30°$. Apart for the transverse shear modulus (G_{23}) in Table 4 and the longitudinal Young's modulus (E_1) in Table 5, the remaining material constants employed are those shown in Eq. (36). Table 4 reveals that the percentage discrepancy between the $PSDPT_{cs}$ and the $PSDPT_{ds}$ frequencies is zero when $G_{23} = G_{13}$. This is due to the fact that, in this case, there is no discontinuity of interlaminar transverse shear stresses and, therefore, both models are equivalent. However, the percentage discrepancy of corresponding results obtained by the two models becomes more evident with decreasing the ratio G_{23}/E_2. This discrepancy never exceeds 1%, in the case of two layers, but can proceed beyond 2% in the case of 12-layered plates. Similar observations can be drawn from the results compared in Table 5. There, the percentage difference of corresponding frequencies is negligible for small stiffness ratios, namely for cases in which the layers constitution does not deviate considerably from that of an isotropic material, but is again increasing with increasing E_1/E_2. Moreover, the sign of the percentage errors denoted in both Tables 4 and 5 changes from positive to negative, when moving from the two- to the 12-layered plates. This shows again that the $PSDPT_{ds}$ is slightly more accurate in the case of the two-layered plate. The $PSDPT_{cs}$ is however considerably more accurate and should therefore be preferred in the case of the 12-layered plate, in which the afore-mentioned effect of the bending extensional coupling due to lamination is considerably weakening.

In an attempt to verify further the above observations (Tables 1–5), a comparison was decided to be made of a few of the eigenfunctions associated to corresponding eigenvalues of the three models employed

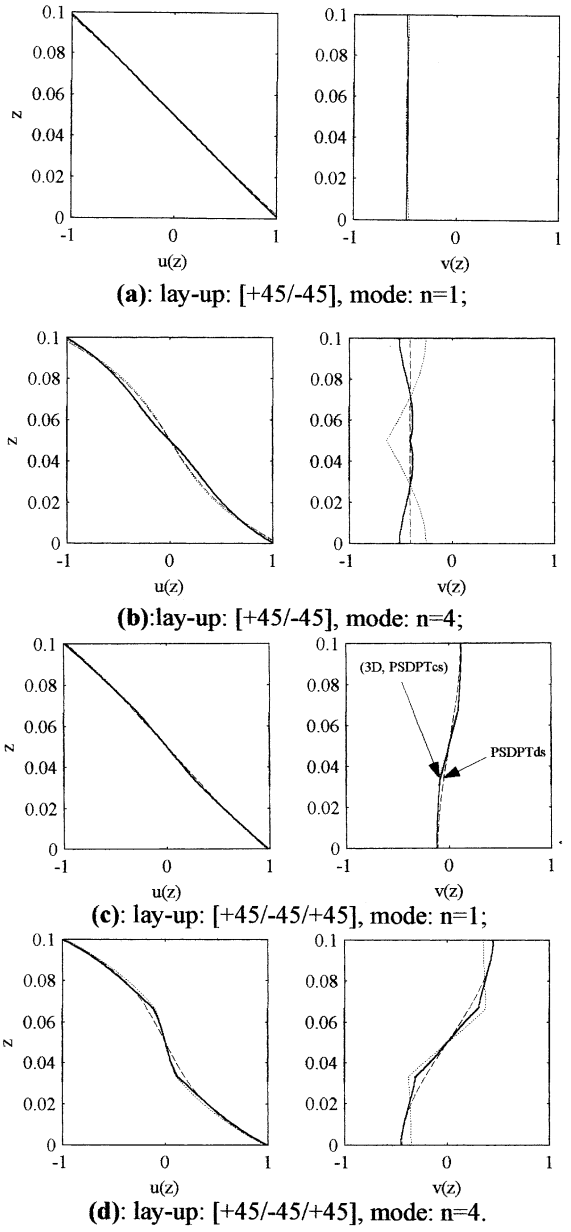

Fig. 3. (a–d) Shapes of in-plane eigenfunction components through the thickness of the laminate (refer Table 3). $PSDPT_{ds}$ (- - -), $PSDPT_{cs}$ (· · ·), 3D (—).

($PSDPT_{ds}$, $PSDPT_{cs}$, 3D). This comparison was realised by scaling the corresponding eigenfunctions until a reasonable graphic match was obtained. The *w*-part of mode shapes displayed is thus not shown, in all of the cases considered in Fig. 3, due to the excellent match achieved for both of the 2D and the exact 3D

eigenfunctions. Hence, the displayed comparisons are attempted by plotting the through-thickness distribution of the in-plane components only of corresponding mode shapes. Accordingly, Fig. 3 depicts the in-plane parts of the eigenfunctions that correspond to certain the particular natural frequencies reported in Table 3. In more detail, Fig. 3(a–d) deal with laminates having an antisymmetric and a symmetric stacking pattern, respectively. These figures show clearly that the 2D model that yields the most accurate natural frequency is always the one that achieves the smallest in-plane displacement deviation from its exact 3D elasticity counterpart. Hence, as was expected after the afore-mentioned observations, the most successful of the two 2D models is the $PSDPT_{ds}$ in the case of a two-layered lay-up (Fig. 3(a) and (b)) and the $PSDPT_{cs}$ in the case of a three-layered symmetric lay-up (Fig. 3(c) and (d)). These observations suggest that there may be a need to look for new shape functions that could model more accurately the in-plane displacement distributions through the thickness of laminates with a small number of layers arranged in an antisymmetric lay-up.

6. Closure

This paper presented a 2D theory that uses only five unknown displacement functions and is able to account for the continuity of interlaminar shear stresses in laminated plates made of monoclinic elastic layers placed in a general, arbitrary, stacking pattern. The governing equations of motion have been obtained by using a new generalised vectorial approach (Soldatos, 1993) but also by applying Hamilton's principle, which made also available the full set of relevant variationally consistent sets of edge boundary conditions. The effectiveness of this 2D dynamical model was verified by employing a certain type of shape functions that are used quite frequently in this kind of dynamic analyses (see Eq. (34)), and comparing its natural frequency predictions with corresponding predictions due to an exact 3D elasticity analysis. This is essentially the dynamic extension of the corresponding, static, cylindrical bending solution due to Pagano (1970).

These comparisons revealed that this specific version of the new model is more accurate than its 2D counterpart that violates continuity of interlaminar stresses, at least in cases of angle-ply laminates that do not exhibit strong bending–extension coupling due to lamination. This observation that, when dealing with cross-ply laminates, was also pointed out in Messina and Soldatos (1999a), is clearly in favour of the present model in many practical situations in which this bending–stretching coupling is zero or very small. Examples of such practical situations refer to multilayered laminate constructions, the very many layers of which are arranged in either a symmetric or even an antisymmetric angle-ply (or cross-ply) lay-up. It is however believed that the present model can be further improved in cases that, as the afore-mentioned two-layered antisymmetric cross- or angle-ply examples, the laminate considered exhibits a strong bending–extension coupling. This may be achieved by searching for new shape functions that could fit better the actual in-plane displacement distributions through the thickness of an antisymmetric laminate with a small number of layers.

Acknowledgements

The work reported in this paper is part of a research European joint project based on a grant awarded to the authors by the Royal Society of London.

Appendix A

The non-zero elements of the matrix $[G]$ that appears in Eq. (27) are as follows:

$$
\begin{aligned}
&G_{14} = G_{25} = G_{36} = 1,\\
&G_{41} = (\lambda^2 C_{44} - m^2(C_{11}C_{44} - C_{16}C_{45}))/g, \quad G_{42} = (-\lambda^2 C_{45} + m^2(C_{45}C_{66} - C_{16}C_{44}))/g,\\
&G_{51} = (-\lambda^2 C_{45} + m^2(C_{45}C_{11} - C_{16}C_{55}))/g, \quad G_{52} = (\lambda^2 C_{55} - m^2(C_{55}C_{66} - C_{16}C_{45}))/g,\\
&G_{46} = m(C_{44}(C_{13} + C_{55}) - C_{45}(C_{45} + C_{36}))/g, \quad G_{56} = m(C_{55}C_{36} + C_{45}C_{13})/g,\\
&G_{63} = (-\lambda^2 + m^2 C_{55})/C_{33}, \quad G_{64} = m(C_{13} + C_{55})/C_{33}, \quad G_{65} = m(C_{36} + C_{45})/C_{33},
\end{aligned}
\tag{A.1}
$$

where $\lambda^2 = \omega^2\rho$ and $g = C_{45}^2 - C_{55}C_{44}$.

References

Bhimaraddi, A., Stevens, L.K., 1984. A high-order theory for free vibration of orthotropic, homogeneous, and laminated rectangular plates. Journal of Applied Mechanics 51, 195–198.

Cho, M., Parmerter, R.R., 1992. An efficient higher-order plate theory for laminated composites. Composite Structures 20, 113–123.

Cho, M., Parmerter, R.R., 1993. Efficient higher-order composite plate theory for general laminated configurations. American Institute of Aeronautics and Astronautics Journal 31, 1299–1306.

Chou, P.C., Carleone, J., 1973. Transverse shear in laminated plate theories. American Institute of Aeronautics and Astronautics Journal 11, 1333–1336.

Di Sciuva, M., 1986. Bending, vibration and buckling of simply supported thick multilayered orthotropic plates: an evaluation of a new displacement model. Journal of Sound and Vibration 105, 425–442.

Di Sciuva, M., 1987. An improved shear-deformation theory for moderately thick multilayered anisotropic shells and plates. Journal of Applied Mechanics 54, 589–596.

Di Sciuva, M., 1992. Multilayered anisotropic plate models with continuous interlaminar stresses. Composite Structures 22, 149–167.

Fan, J., Ye, J., 1990. An exact solution for the static and dynamics of laminated thick plates with orthotropic layers. International Journal of Solids and Structure 26, 655–662.

He, J.-F., Chou, M., Zhang, X., 1993. Bending analysis of laminated plates using a refined shear deformation theory. Composite Structures 24, 125–138.

He, J.-F., Ma, B.-A., 1994. Vibration analysis of laminated plates using a refined shear deformation theory. Journal of Sound and Vibration 175, 577–591.

Jones, R.M., 1975. Mechanics of Composite Materials. Hemisphere, New York.

Lee, K.H., Lin, W.Z., Chow, S.T., 1994. Bidirectional bending of laminated composite plates using an improved zig-zag model. Composite structures 28, 283–294.

Lee, K.H., Senthilnathan, N.R., Lim, S.P., Chow, S.T., 1990. An improved zig-zag model for the bending of laminated composite plates. Composite Structures 15, 137–148.

Lee, K.H., Xavier, P.B., Chew, C.H., 1993. Static response of unsymmetric sandwich beams using an improved zig-zag model. Composites Engineering 3, 235–248.

Librescu, L., Lin, W., 1996. Two models of shear deformable laminated plates and shells and their use in prediction of global response behavior. European Journal of Mechanics A/Solids 15, 1095–1120.

Librescu, L., Lin, W., 1999. Non-linear response of laminated plates and shells to thermomechanical loading: implications of violation of interlaminar shear traction continuity requirement. International Journal of Solids and Structures 36, 4111–4147.

Librescu, L., Lin, W., Sciuva, M., Icardi, U., 1997. Postbuckling of laminated composite and sandwich plates and shells: on the significance of the fulfilment of the static interlayer continuity conditions. Computer Methods in Applied Mechanics and Engineering 148, 165–186.

Messina, A., Soldatos, K.P., 1999a. Influence of edge boundary conditions on the free vibrations of cross-ply laminated circular cylindrical panels. The Journal of the Acoustical Society of America 106, 2608–2620.

Messina, A., Soldatos, K.P., 1999b. Ritz-type dynamic analysis of cross-ply laminated circular cylinders subjected to different boundary conditions. Journal of Sound and Vibration 227, 749–768.

Pagano, N.J., 1969. Exact solutions for composite laminates in cylindrical bending. Journal of Composite Materials 3, 398–411.

Pagano, N.J., 1970. Influence of shear coupling in cylindrical bending of anisotropic laminates. Journal of Composite Materials 4, 330–343.

Reddy, J.N., 1984. A simple higher-order theory for laminated composite plates. Journal of Applied Mechanics 51, 745–752.
Ren, J.G., 1986a. A new theory of laminated plate. Composite Science and Technology 26, 225–239.
Ren, J.G., 1986b. Bending theory of laminated plate. Composite Science and Technology 27, 225–248.
Ren, J.G., Owen, D.R.J., 1989. Vibration and Buckling of laminated plates. International Journal of Solids and Structures 25, 95–106.
Savithri, S., Varadan, T.K., 1990a. Accurate bending analysis of laminated orthotropic plates. American Institute of Aeronautics and Astronautics Journal 28, 1842–1844.
Savithri, S., Varadan, T.K., 1990b. Free vibration and stability of cross-ply laminated plates. Journal of Sound and Vibration 141, 516–520.
Soldatos, K.P., 1988. On certain refined theories for plate bending. Journal of Applied Mechanics 55, 994–995.
Soldatos, K.P., 1993. Vectorial approach for the formulation of variationally consistent higher-order plate theories. Composites Engineering 3, 3–17.
Soldatos, K.P., Timarci, T., 1993. A unified formulation of laminated composite, shear deformable, five-degrees-of-freedom cylindrical shell theories. Composite Structures 25, 165–171.
Soldatos, K.P., Messina, A., 1998. Vibration studies of cross-ply laminated shear deformable circular cylinders on the basis of orthogonal polynomials. Journal of Sound and Vibration 218, 219–243.
Soldatos, K.P., Ye, J.Q., 1995. Axisymmetric static and dynamic analysis of laminated hollow cylinders composed of monoclinic elastic layers. Journal of Sound and Vibration 184, 245–259.
Sun, C.T., Whitney, J.M., 1973. Theories for the dynamic response of laminated plates. American Institute of Aeronautics and Astronautics Journal 11, 178–183.
Timarci, T., Soldatos, K.P., 1995. Comparative dynamic studies for symmetric cross-ply circular cylindrical shells on the basis of a unified shear deformable shell theory. Journal of Sound and Vibration 187, 609–624.
Timarci, T., Soldatos, K.P., 2000. Vibrations of angle-ply laminated circular cylindrical shells subjected to different sets of edge boundary conditions. Journal of Engineering Mathematics 37, 211–230.
Whitney, J.M., 1987. Structural analysis of laminated anisotropic plates. Technomic, Lancaster, PA.
Whitney, J.M., Pagano, N.J., 1970. Shear deformation in heterogeneous anisotropic plates. Journal of Applied Mechanics 37, 1031–1036.
Yang, P.C., Norris, C.H., Stavsky, Y., 1966. Elastic wave propagation in heterogeneous plates. International Journal of Solids and Structures 2, 665–684.